Dual-energy Computed Tomography (DECT) Scan for Determination of Renal Stone Composition: A Phantom Study

Mahboobeh Sheikhi [1, 2], Sedigheh Sina [1, 3, *] and Mehrnoosh Karimipourfard [1]

[1]School of Mechanical Engineering, Shiraz University, Shiraz, Iran
[2]Abu Ali Sina Hospital, Shiraz, Iran
[3]Radiation Research Center, Shiraz University, Shiraz, Iran

[*] *Corresponding author*: School of Mechanical Engineering, Shiraz University, Shiraz, Iran. Email: samirasina@yahoo.com

Abstract

Background: Dual-energy computed tomography (DECT) scan has been proposed as an effective modality for determining the chemical composition of renal stone subtypes.
Objectives: This study aimed to evaluate and compare the efficacy of DECT in the identification of renal stone type and composition versus biochemical analysis as the gold standard.
Materials and Methods: The type of 146 renal stones, removed from patients by surgery, was determined in a medical laboratory. The stones were then inserted into the kidney of an anthropomorphic Rando phantom, and DECT scans were acquired. The stone type, specified by the scanner software, was compared with the results of biochemical analysis as the gold standard.
Results: The DECT scans showed acceptable accuracy in identifying the chemical composition of renal stone subtypes. Based on the comparison of biochemical analysis and DECT results, the accuracy values for cystine, uric acid, and calcium-oxalate stones were 97%, 100%, and 97%, respectively.
Conclusion: Based on the present results, DECT could detect pure uric acid, cystine, and calcium-oxalate stone types with high sensitivity. However, for mixed stones, the stone type, directly identified by DECT scan, was not reliable.

Keywords: Dual-energy CT, Renal Stone, Composition

1. Background

The prevalence of renal stones is increasing in different countries around the world. In Iran, a high prevalence of renal stones (~ 5.7%) has been reported (1-3). The identification of renal stone subtypes is crucial for planning effective therapeutic and preventive strategies (4, 5). For instance, uric acid (UA) stones are commonly treated or even prevented by dietary modifications, while cystine (Cys) stones are treated using endoscopic methods (6).

The stone type analysis is commonly performed in chemical laboratories. Infrared spectroscopy, X-ray diffraction, and polarized light microscopy are the three most common in vitro techniques for determining the stone type. However, these methods are time-consuming and costly. Also, such methods can be only performed after the extraction of stones from the body. Therefore, chemical methods are not beneficial for preoperative treatment planning (7).

Currently, abdominal-pelvic computed tomography (CT) scan has been employed as the standard in vivo method for the detection of urinary stones (8). Nevertheless, determination of stone composition cannot be performed by single-energy CT scan. Dual-energy CT (DECT) scanning, which is known as one of the most promising developments in radiology, is used for determining the components of different materials or material identification (9). Several studies have reported the clinical benefits of DECT in the identification of renal stone types (10-16).

2. Objectives

This study aimed to examine the ability of DECT in determining the chemical composition of renal stone subtypes. For this purpose, different renal stones were scanned via kilovoltage (kV)-switching DECT, and the stone subtypes identified by DECT were compared with the results of biochemical analysis.
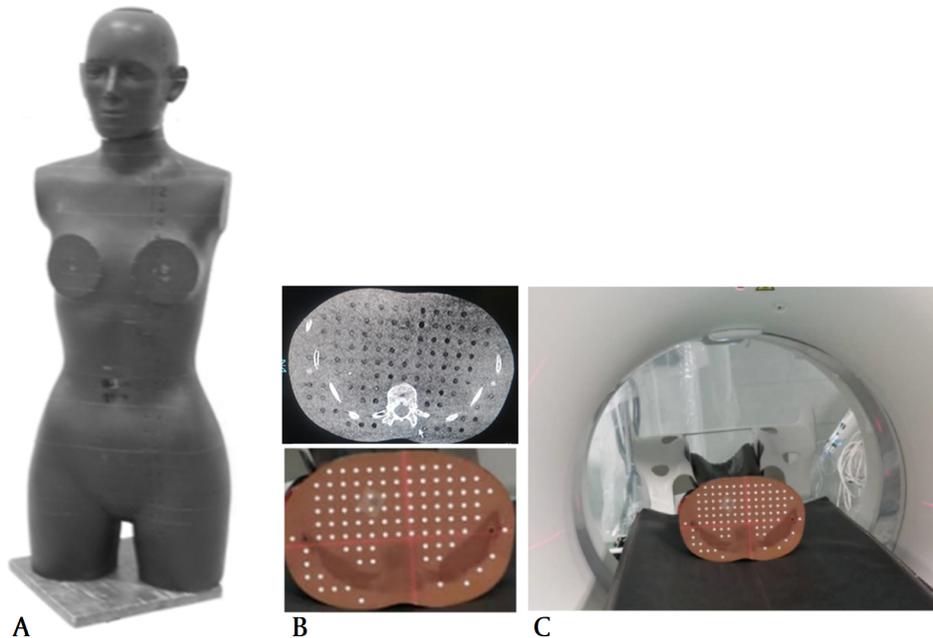
Figure 1. A, The Alderson Rando phantom; B, A typical CT image; C, Imaging of the phantom.

3. Materials and Methods

3.1. Stone Samples

A total of 156 renal stones, which were removed from patients by surgery and sent to the biochemistry laboratory for determination of their subtype, were examined in this study. Four stone types were distinguished based on the results of biochemical analysis, including Cys, uric acid (UA), calcium-oxalate (CaOx), and mixed stones.

3.2. Dual-energy CT Acquisition

The renal stones were inserted into the kidney of an anthropomorphic female Alderson Rando phantom, and DECT scans were acquired using a single-source DECT scanner (Toshiba Aquilion Prime One, Toshiba, Japan). Until now, various strategies have been proposed for DECT scanning, including kV switching with a single source and detector, scanning with one source and dual-layer detectors, and scanning with dual sources and dual detectors. Generally, the Alderson Rando phantom is an anthropomorphic phantom composed of tissue equivalent materials, which is commonly used for clinical dosimetry; therefore, the CT scan of this phantom resembles that of a real human [17, 18]. The female Rando phantom used in this study simulated a 163-cm-tall woman, weighing 54 kg (Figure 1).

Stones with a size smaller than 3.0 mm were selected so that they could be inserted into the holes of the phantom.

Two scans were acquired based on the routine procedure used for imaging patients with renal stones. First, ultra-low-dose scanning was performed based on the single-energy protocol of the CT unit. Commonly, ultra-low-dose scanning of the abdomen is performed with a large field of view to determine the exact location of the stone in the body. Next, single-source, dual-energy, rapid-kVp-switching CT scan was performed for distinguishing the stone type.

The adaptive iterative dose reconstruction 3D (AIDR 3D) technique was applied in the Toshiba CT scanner to obtain ultra-low-dose scans while maintaining the image quality. This reconstruction method is known as an important evolution in Toshiba CT scanners [19]. Based on the information obtained by the dose report of the CT scanner, the radiation dose can be reduced 10 times in ultra-low-dose CT scanning compared to conventional CT scans. The imaging technique used for image acquisition was as follows:

Peak tube voltage of 120 kV and 15 mAs for ultra-low-dose CT scanning with AIDR 3D reconstruction technique.

Peak tube voltage of 80 kV and 92 mAs for low-energy DECT.

Peak tube voltage of 135 kV and 15 mAs for high-energy

DECT.

Single-photon CT scanning is regarded as an accurate method for renal stone detection. However, the stone type cannot be accurately determined using this method. Therefore, the attenuation ratio (AR) or the Hounsfield unit (HU) ratio of low- and high-energy DECT was used for determining the stone type (Equation 1):

$$Attenuation\ ratio\ (AR) = \frac{HU\ in\ low\ energy\ (or\ low\ kVp)}{HU\ in\ high\ energy\ (or\ high\ kVp)}$$

(1)

Finally, the attenuation and AR values of low-energy (80 kVp) and high-energy (135 kVp) X-ray imaging were used in DECT scanners to determine the chemical composition of renal stone subtypes.

3.3. Statistical Analysis

The DECT scans of the Rando phantom were used for determining the renal stone subtypes. The mean values and standard deviations (SDs) of HU, as well as the AR values of stone images, were extracted from the CT scans using low- and high-energy X-rays. The box and whisker plots were employed for analyzing the AR values. The box and whisker plots allow for the comparison of data from different categories for a better decision-making. Such easy-to-interpret plots can summarize the AR data for multiple stones and display multiple results in a single graph. The mean, median, minimum, maximum, Q1, and Q3 values are shown in a single plot in this study.

To assess the significance of the mean values of AR for different renal stone subtypes, *t*-test was used, and a P-value less than 0.05 was considered statistically significant. Finally, the area under the receiver operating characteristic (ROC) curve (AUC) was measured to determine the performance of DECT in stone type classification. After determining the stone type using a DECT scanner, the diagnostic value of DCET was examined by estimating the sensitivity, specificity, and accuracy of DECT results. The biochemical analysis results were used as the gold standard for determining the efficacy of DECT in identifying the type of renal stones.

4. Results

4.1. Dual-energy CT for Determination of Pure Stone Types

The results of biochemical analysis indicated 110 pure stones, 40 UA stones, 41 Cys stones, and 29 CaOx stones. The size of stones in their largest section was 3 mm, while in some sections of stones, thicknesses < 3 mm were observed, as the stones did not have a regular geometric shape. The size variations measured in different sections of pure and mixed stone types are presented in Table 1.

Based on the comparison of the results of biochemical analysis and DECT, the diagnostic accuracy for Cys, UA, and CaOx stones was estimated at 97%, 100%, and 97% respectively, indicating the repeatability of DECT scans. The results pertaining to the sensitivity, specificity, and accuracy of DECT are shown in Table 2.

Figure 2A presents the X-ray attenuations of low-kVp X-ray versus high-kVp X-ray. Table 3 also indicates the mean values, SDs, and range of HU in both low- and high-energy X-rays for different stones. Moreover, Figure 2B presents the boxplot of attenuation (AR) or HU ratio for the three stone types. Based on the results, the average ARs were 1.00 ± 0.06, 1.27 ± 0.03, and 1.39 ± 0.06 for the UA, Cys, and CaOx stones, respectively.

Additionally, *t*-test was used to assess the significance of the mean AR values. According to the P-values (< 0.05), the ARs of different stones were statistically significant. The minimum, maximum, and median values of AR are also shown in Figure 2B. Such differences in the AR values were used in DECT for the identification of stone types. The AUCs for the Cys, UA, and CaOx stones were measured to be 0.970 (95% CI: 0.872 - 0.998), 0.980 (95% CI: 0.899 - 0.996), and 0.975 (95% CI: 0.885 - 0.995), respectively.

4.2. Dual-energy CT for Determination of Mixed Stone Types

Based on the results of biochemical analysis, 46 stones were identified as a combination of different stone types. Overall, 32 stones contained a high calcium content (> 70%). According to Table 4, DECT classified all these 32 stones as CaOx.

Based on the results of biochemical analysis, there were nine mixed stones, composed of 60% UA and 40% CaOx. The DECT yielded different results for these stones. According to DECT, five stones were distinguished as UA, two as CaOx, and three as Cys stones. Finally, five stones, which were reported to contain a mixture of 50% calcium, 40 - 45% UA, and 5 - 10% ammonium according to the biochemical analysis, were misidentified as Cys stones.

5. Discussion

This phantom study was performed to identify the chemical composition of renal stones using DECT. The comparison of these results with the findings of biochemical laboratory analysis showed that DECT could determine the type of pure stones with high sensitivity.
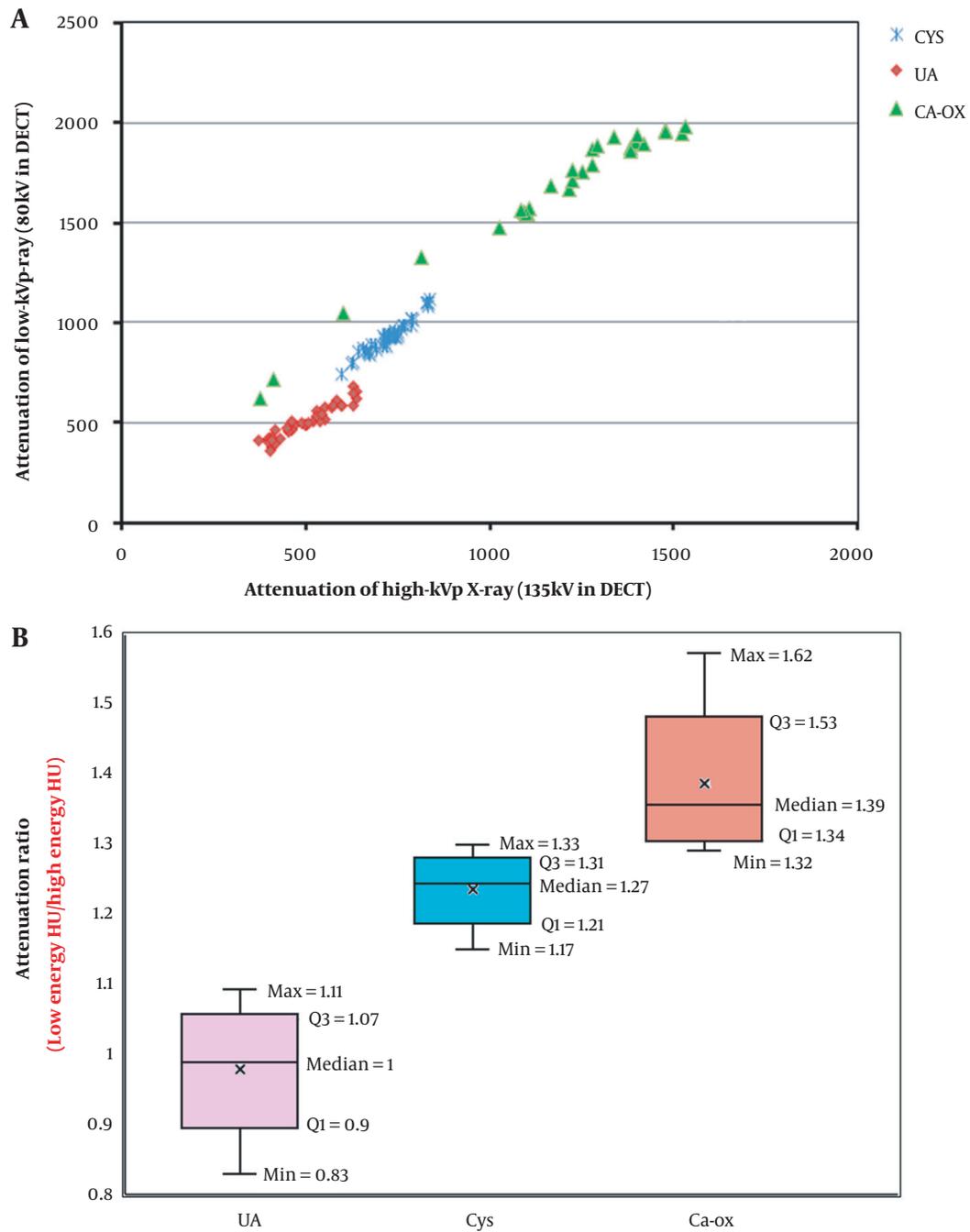
Figure 2. A, The X-ray attenuation values in low- and high-energy X-rays for pure renal stones. B, The attenuation ratio (AR) for the renal stones (n = 101) examined in this study.

Table 1. Characteristics of Renal Stones in This Study

	UA	CaOx	Cys	Mixed stones
No.	40	29	41	46
Diameter, mm: mean (min - max)	1.9 (0.9 - 2.9)	2.1 (1.0 - 3.0)	2.1 (0.9 - 3.0)	2.9 (1.8 - 3)

Abbreviations: UA, uric acid; CaOx, calcium-oxalate; Cys, cystine.

Table 2. Diagnostic Indices of DECT in Determining the Stone Type and 95% Confidence Intervals (CIs)

	Cys	UA	CaOx
Accuracy	0.97 (0.94 - 0.99)	1.00 (1.00 - 1.00)	0.97 (0.94 - 0.99)
Sensitivity	0.95 (0.92 - 0.98)	1.00 (1.00 - 1.00)	0.97 (0.94 - 0.99)
Specificity	0.98 (0.970 - 0.99)	0.96 (0.93 - 0.99)	0.98 (0.96 - 0.99)
Positive predictive value	0.97 (0.95 - 0.99)	0.98 (0.96 - 0.99)	0.96 (0.93 - 0.99)

Abbreviations: DECT, dual-energy computed tomography; UA, uric acid; CaOx, calcium-oxalate; Cys, cystine.

Table 3. Variations in Attenuation (HU) Values at High and Low Energy Levels

Type of renal stone/energy	Range, min-max	Mean ± SD
Cys		
High energy	745 - 1114	938.28 ± 80.13
Low energy	600 - 836	731.53 ± 55.42
UA		
High energy	360 - 684	503 ± 82.97
Low energy	371 - 639	501.38 ± 80.75
CaOx		
High energy	617 - 1978	1653.68 ± 354.28
Low energy	377 - 1532	1178.25 ± 302.81

Abbreviations: HU, Hounsfield unit; Cys, cystine; UA, uric acid; CaOx, calcium-oxalate.

Table 4. Stone Type Determination by DECT for Stones with a High Calcium Content

Number of stones	Chemical analysis results	Renal stone type according to DECT
20	80% CaOx; 20% calcium-phosphate	CaOx
3	70% CaOx; 30% UA	CaOx
5	70% CaOx; 5% calcium-phosphate; 25% other types	CaOx
4	60% CaOx; 20% calcium-phosphate; 20% other types	CaOx

Abbreviations: DECT, dual-energy computed tomography; CaOx, calcium-oxalate; UA, uric acid.

Generally, AUC is a scoring value, which can determine the extent to which classifiers are capable of distinguishing different subtypes. An excellent classifier has an AUC close to one, which means it has a good measure of separability. Based on the results of this study, the AUCs for the three stone types were close to one (> 0.97). It can be concluded that DECT is an acceptable classifier for pure renal stones. The high values of sensitivity, accuracy, and specificity also confirmed the validity of DECT results.

The basis of stone type determination is the difference in the attenuation and AR values of different renal stones. The present results revealed significant differences in the AR values of different stones. However, for mixed stone types, DECT cannot accurately represent the stone type. Based on the present results, the stone type is identified as CaOx when its calcium content is high. For instance, if the calcium content is higher than 70%, DECT distinguishes the stones as CaOx. For stones which are a mixture of several stone types, the results of DECT were completely inaccurate. Overall, the present results are consistent with the findings of previous research ([13]-[15]). In conclusion, based on the results of this brief research, for an accurate detection of all pure and mixed renal stones, further analytical methods are needed. In future studies, we wish to extend

our work to automatic component identification of pure and mixed renal stone subtypes based on deep neural networks.

Footnotes

References

1. Safarinejad MR. Adult urolithiasis in a population-based study in Iran: prevalence, incidence, and associated risk factors. *Urol Res*. 2007;**35**(2):73–82. [PubMed ID: 17361397]. https://doi.org/10.1007/s00240-007-0084-6.

2. Farshid S, Aghdashi A, Fallahi H, Valizadeh R, Rahimi MM. Evaluation of Osteoporosis Frequency in Patients With Recurrent Kidney Stones. *Acta Med Iran*. 2020:494–9. https://doi.org/10.18502/acta.v58i10.4911.

3. Khalili P, Jamali Z, Sadeghi T, Esmaeili-Nadimi A, Mohamadi M, Moghadam-Ahmadi A, et al. Risk factors of kidney stone disease: a cross-sectional study in the southeast of Iran. *BMC Urol*. 2021;**21**(1):141. [PubMed ID: 34625088]. [PubMed Central ID: PMC8499392]. https://doi.org/10.1186/s12894-021-00905-5.

4. Worcester EM, Coe FL. Nephrolithiasis. *Prim Care*. 2008;**35**(2):369–91. vii. [PubMed ID: 18486720]. [PubMed Central ID: PMC2518455]. https://doi.org/10.1016/j.pop.2008.01.005.

5. Ferrari P, Bonny O. [Diagnosis and prevention of uric acid stones]. *Ther Umsch*. 2004;**61**(9):571–4. [PubMed ID: 15493118]. https://doi.org/10.1024/0040-5930.61.9.571.

6. Karki N, Leslie SW. *Struvite And Triple Phosphate Renal Calculi*. StatPearls [Internet]; 2022.

7. Hidas G, Eliahou R, Duvdevani M, Coulon P, Lemaitre L, Gofrit ON, et al. Determination of renal stone composition with dual-energy CT: in vivo analysis and comparison with x-ray diffraction. *Radiology*. 2010;**257**(2):394–401. [PubMed ID: 20807846]. https://doi.org/10.1148/radiol.10100249.

8. Tsili AC, Varkarakis I, Pasoglou V, Anagnostou N, Argyropoulou MI. CT of the urinary tract revisited. *Eur J Radiol*. 2023;**160**:110717. [PubMed ID: 36773595]. https://doi.org/10.1016/j.ejrad.2023.110717.

9. Akisato K, Nishihara R, Okazaki H, Masuda T, Hironobe A, Ishizaki H, et al. Dual-Energy CT of Material Decomposition Analysis for Detection with Bone Marrow Edema in Patients with Vertebral Compression Fractures. *Acad Radiol*. 2020;**27**(2):227–32. [PubMed ID: 30876711]. https://doi.org/10.1016/j.acra.2019.02.015.

10. Li ZX, Jiao GL, Zhou SM, Cheng ZY, Bashir S, Zhou Y. Evaluation of the chemical composition of nephrolithiasis using dual-energy CT in Southern Chinese gout patients. *BMC Nephrol*. 2019;**20**(1):273. [PubMed ID: 31324154]. [PubMed Central ID: PMC6642481]. https://doi.org/10.1186/s12882-019-1441-8.

11. Ilyas M, Dev G, Gupta A, Bhat TA, Sharma S. Dual-energy computed tomography: A reliable and established tool for In vivo differentiation of uric acid from nonuric acid renal Stones. *Niger Postgrad Med J*. 2018;**25**(1):52–9. [PubMed ID: 29676347]. https://doi.org/10.4103/npmj.npmj_24_18.

12. Rompsaithong U, Jongjitaree K, Korpraphong P, Woranisarakul V, Taweemonkongsap T, Nualyong C, et al. Characterization of renal stone composition by using fast kilovoltage switching dual-energy computed tomography compared to laboratory stone analysis: a pilot study. *Abdom Radiol (NY)*. 2019;**44**(3):1027–32. [PubMed ID: 30259102]. https://doi.org/10.1007/s00261-018-1787-6.

13. Basha MAA, AlAzzazy MZ, Enaba MM. Diagnostic validity of dual-energy CT in determination of urolithiasis chemical composition: In vivo analysis. *Egypt J Radiol Nucl Med*. 2018;**49**(2):499–508. https://doi.org/10.1016/j.ejrnm.2017.12.018.

14. Kapanadze LB, Rudenko VI, Serova NS, Rapoport LM, Aleksandrova KA, Novikov AA. [Dual-energy computed tomography in the diagnostics of urolithiasis]. *Urologiia*. 2019;(5):31–6. Russian. [PubMed ID: 31808629].

15. Singh A, Khanduri S, Khan N, Yadav P, Husain M, Khan AU, et al. Role of Dual-Energy Computed Tomography in Characterization of Ureteric Calculi and Urinary Obstruction. *Cureus*. 2020;**12**(5). e8002. [PubMed ID: 32528744]. [PubMed Central ID: PMC7279691]. https://doi.org/10.7759/cureus.8002.

16. Magistro G, Bregenhorn P, Krauss B, Norenberg D, D'Anastasi M, Graser A, et al. Optimized management of urolithiasis by coloured stent-stone contrast using dual-energy computed tomography (DECT). *BMC Urol*. 2019;**19**(1):29. [PubMed ID: 31039768]. [PubMed Central ID: PMC6492318]. https://doi.org/10.1186/s12894-019-0459-3.

17. Bao J, Chen L, Zhu JH, Fei ZF, Hu ZT, Wang HZ, et al. Comprehensive end-to-end test for intensity-modulated radiation therapy for nasopharyngeal carcinoma using an anthropomorphic phantom and EBT3 film. *Int J Radiat Res*. 2021;**19**(1):31–9. https://doi.org/10.29252/ijrr.19.1.31.

18. Farajzadeh E, Sina S. Developing a radiochromic dosimeter for dosimetry in blood irradiation chambers. *Radiat Phys Chem*. 2021;**188**:109637. https://doi.org/10.1016/j.radphyschem.2021.109637.

19. Maamoun I, Khalil MM. Assessment of iterative image reconstruction on kidney and liver donors: Potential role of adaptive iterative dose reduction 3D (AIDR 3D) technology. *Eur J Radiol*. 2018;**109**:124–9. [PubMed ID: 30527293]. https://doi.org/10.1016/j.ejrad.2018.10.020.